Biochimica et Biophysica Acta 1788 (2009) 122–135

Contents lists available at ScienceDirect

Biochimica et Biophysica Acta

journal homepage: www.elsevier.com/locate/bbamem

Review

Atom-scale molecular interactions in lipid raft mixtures

Perttu S. Niemelä [a], Marja T. Hyvönen [b], Ilpo Vattulainen [a,c,d,*]

[a] Laboratory of Physics, Helsinki University of Technology, Finland
[b] Wihuri Research Institute, Finland
[c] Department of Physics, Tampere University of Technology, Finland
[d] MEMPHYS—Center for Biomembrane Physics, University of Southern Denmark, Denmark

ARTICLE INFO

Article history:
Received 26 June 2008
Received in revised form 18 August 2008
Accepted 21 August 2008
Available online 6 September 2008

Keywords:
Lipid
Raft
Membrane
Bilayer
Sphingomyelin
Sterol
Cholesterol
Phosphatidylcholine
Molecular dynamics
Simulation

ABSTRACT

We review the relationship between molecular interactions and the properties of lipid environments. A specific focus is given on bilayers which contain sphingomyelin (SM) and sterols due to their essential role for the formation of lipid rafts. The discussion is based on recent atom-scale molecular dynamics simulations, complemented by extensive comparison to experimental data. The discussion is divided into four sections. The first part investigates the properties of one-component SM bilayers and compares them to bilayers with phosphatidylcholine (PC), the focus being on a detailed analysis of the hydrogen bonding network in the two bilayers. The second part deals with binary mixtures of sterols with either SM or PC. The results show how the membrane properties may vary substantially depending on the sterol and SM type available, the membrane order and interdigitation being just two of the many examples of this issue. The third part concentrates on the specificity of intermolecular interactions in three-component mixtures of SM, PC and cholesterol (CHOL) under conditions where the concentrations of SM and CHOL are dilute with respect to that of PC. The results show how SM and CHOL favor one another, thus acting as nucleation sites for the formation of highly ordered nanosized domains. Finally, the fourth part discusses the large-scale properties of raft-like membrane environments and compares them to the properties of non-raft membranes. The differences turn out to be substantial. As a particularly intriguing example of this, the lateral pressure profiles of raft-like and non-raft systems indicate that the lipid composition of membrane domains may have a major impact on membrane protein activation.
© 2008 Elsevier B.V. All rights reserved.

Contents

* Corresponding author. Department of Physics, Tampere University of Technology, P.O. Box 692, FI-33101 Tampere, Finland. Tel.: +358 9 451 5805; fax: +358 9 451 3116.
E-mail address: Ilpo.Vattulainen@tut.fi (I. Vattulainen).

0005-2736/$ – see front matter © 2008 Elsevier B.V. All rights reserved.
doi:10.1016/j.bbamem.2008.08.018

1. Introduction

It is difficult to overestimate the importance of membranes for life, considering that they surround all cells and organelles and control everything that goes in or out of them. The backbone of any membrane is a lipid bilayer, a soft interface that is only a few nanometers thick. Despite their seemingly simple nature, membranes are astonishingly complex in terms of their structure as well as the time and length scales associated with membrane processes. Just as an example, the number of lipid species in biomembranes is over 1000 in total [1], and in erythrocytes alone this number is about 100 [2]. Another example are the length scales of lipids and lipid complexes that range from nanometers to microns, together with the time scales of dynamic processes that cover picoseconds to weeks or months, the latter related to the typical lifetime of a cell. One major question of membrane research is to explain the underlying biological reasons of this variety.

Our view of the role of lipids in biological membranes has changed in the past 30 years since the introduction of the fluid-mosaic model by Singer and Nicolson [3]. The fluid-mosaic model predicted that cellular membranes are fluid, characterized by a random distribution of molecular components in the membrane, resulting in lateral and rotational freedom. More detailed studies have shown that membranes are not so simple, though. The idea of lateral heterogeneities and domains in simple model membranes was suggested already over three decades ago [4,5], but their possible biological effects, when present in the membranes of living cells, have been understood much more recently after introduction of the lipid raft hypothesis [6–8]. In essence, the lipid raft model stresses the importance of lipids in cellular functions, as membrane proteins do not function alone but act together with the lipids. For example, lipid rafts have been suggested to take part in various dynamic cellular processes such as membrane trafficking, signal transduction, and regulation of the activity of membrane proteins [6–8].

Studies of lipid mixtures in model membranes have lead to the idea that lipid rafts are small (10–200 nm), heterogeneous, highly dynamic, sterol and sphingolipid-enriched domains that compartmentalize cellular processes [9]. In addition to membranes, the existence of sterol–sphingolipid-enriched areas has been suggested in other lipid structures such as the surface of low density lipoproteins [10]. Despite the progress made in the field lately, the understanding of lipid rafts and their properties has not yet been fully clarified. For example, we do not know whether actual phase separation or merely a non-random mixing is the best description of biomembranes [11]. Direct evidence of rafts *in vivo* is mainly based on monitoring the motions of membrane proteins [12–14] or on differential partitioning of fluorescent probes in membrane environments [15]. It is however difficult to perform experiments using living cells, which complicates measurements of physical quantities of rafts, such as their exact lipid composition, characteristic size, and lifetime [16,17]. Another partly unresolved question is the exact nature of the molecular interactions that lead to lipid immiscibilities in membranes [18,19].

In glycerophospholipids, the glycerol backbone facilitates a high variability of different headgroups and acyl chain combinations. The main headgroup classes are phosphocholine (PC), phosphoethanolamine (PE), phosphoserine (PS) and phosphoinositol (PI), of which the two latter are charged [2]. The acyl chains typically vary between 16 and 22 carbons in length and contain 0 to 6 double bonds. Fig. 1A

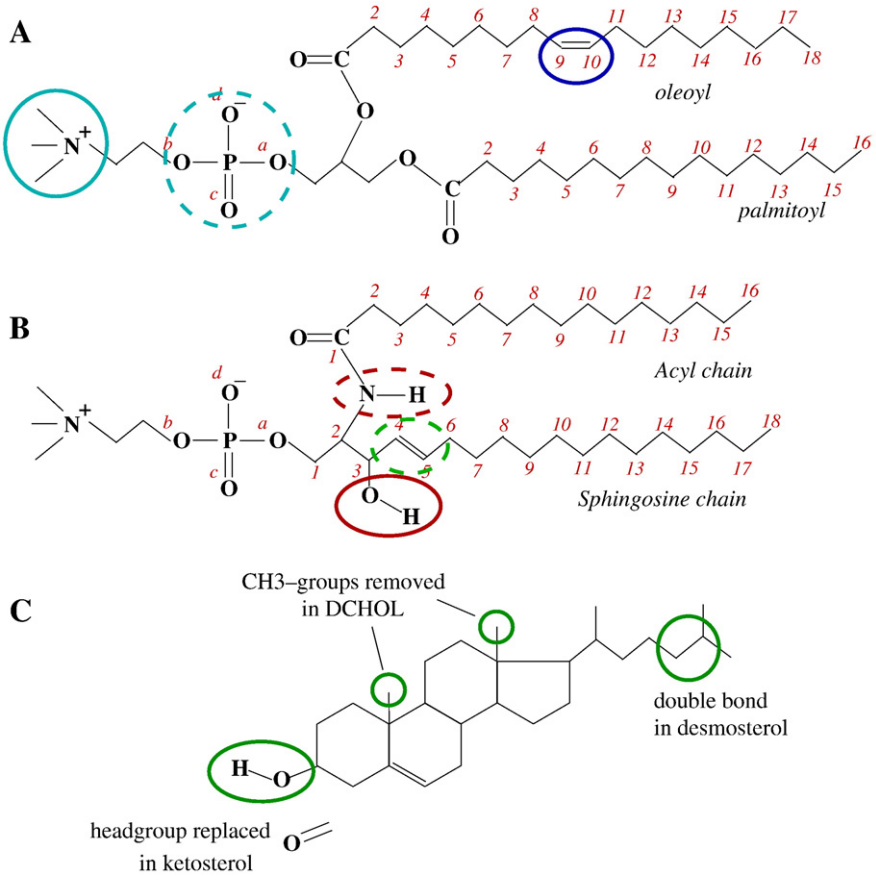

Fig. 1. Molecular structure of three membrane lipids: (A) POPC, (B) palmitoyl-sphingomyelin (PSM), and (C) CHOL. The important functional groups have been indicated with different colors: the phosphate (cyan, dashed) and choline (cyan) of the PC-headgroup, together with the *cis*-double bond (blue) of the monounsaturated chain. The two hydrogen donor groups of SM are the amide group (red dashed) and the hydroxyl group (red). Note also the *trans*-double bond (green, dashed) between the fourth and the fifth carbon of the sphingosine chain of SM, which is lacking in POPC. For CHOL, three modifications are also indicated.

shows a typical glycerophospholipid, the palmitoyl-oleoyl-PC (POPC), which contains the PC-headgroup and two different, ester bonded acyl chains: palmitoyl and oleoyl.

Typical sphingolipids have either the PC-headgroup (sphingomyelin, SM) or a sugar residue (glycosphingolipids). For SM, the headgroup structure and the length of the sphingosine chain are usually fixed, but the length and saturation of the amide-linked acyl chain can vary. In nature, the most common sphingosine base is the 18:1$^{trans\Delta4}$, which is in the D-*erythro* configuration [20]. The most typical acyl chains of SM in different tissues are 16:0, 18:0, 22:0, 24:0, and 24:1$^{cis\Delta15}$ [18]. The population of SM in biological membranes is mainly dominated by very long-chained species (>20 carbons) [21]. Fig. 1B shows the structure of the 16:0-SM (palmitoyl-SM, PSM), which is perhaps the most extensively studied SM in literature.

The molecular structure of SM resembles closely that of PC, but there are a few significant differences [18,22]. In particular, the higher saturation state, the long acyl chains, the *trans*-double bond, and the two polar hydrogens in the hydroxyl and amide moieties of SM are different from PC. Additionally, the double bond of the acyl chain of SM is usually located further away from the headgroup, closer to the bilayer center.

The properties of one-component SM bilayers differ from those of PC bilayers. For example, the area per lipid is usually lower in SM bilayers than in corresponding PC bilayers, which is probably a consequence of the excess hydrogen bonding network in the SM bilayer. Perhaps surprisingly, the main phase transition temperature of PSM (T_m=41 °C) is almost identical to the saturated dipalmitoyl-PC (DPPC) [20,23,24], which is structurally largely similar to SM, the only difference being the glycerol moiety linked to a fatty acid chain instead of the sphingosine chain. However, the insertion of a *cis*-double bond has a more significant effect on the T_m of PC than of SM [23,25], which suggests that the intermolecular hydrogen bonding has an important role to play in the phase behavior of SMs.

The distinct features in the molecular structure of SM may have substantial effects on its interactions with other membrane components such as sterols and proteins. For example, the nature of the SM–CHOL interaction has been proposed to be more attractive when compared with the interactions of CHOL with other lipids [26]. This interaction is usually related to the capacity of SM to form intra- and intermolecular hydrogen bonds [27,28] or to the pronounced attractive interaction between the ring structure of CHOL and chains of SM [19,29]. For the latter, the long and saturated nature of the acyl chains of SM may be crucial, as well as the prevalence of the scarce double bonds further away from the lipid–water interface.

As for sterols, their molecular structure is characterized by the rigid and hydrophobic ring structure, a short flexible chain, and a small polar headgroup [30]. Fig. 1C shows the structure of cholesterol (CHOL), the most common sterol in mammalian membranes. Additionally, the structure of its closest precursor in the synthetic pathway, desmosterol, is also shown together with an artificially demethylated cholesterol (DCHOL) and ketosterol where the hydroxyl group of CHOL is replaced with a keto group. Other major classes of natural sterols are plant sterols and sterol derivates, such as the cholesteryl esters.

The most important function of CHOL is perhaps related to its ability to regulate the physical properties of membranes [31]. For a fluid bilayer, the addition of CHOL leads to increased orientational order of the acyl chains and increased packing density within the bilayer plane. In addition, CHOL decreases the passive permeability of small solutes through the membrane [32,33] and suppresses the lateral diffusion of lipids [34,35]. These effects are largely explained by the tendency of CHOL to accommodate itself into the non-polar region of the acyl chains and to reduce the free volume within that region [35,36].

The ability of CHOL to increase the acyl chain order of liquid bilayers is based on the smooth and bulky hydrophobic body of the CHOL molecule that packs well with hydrocarbon chains [26]. However, the two opposite faces of the ring of CHOL contribute differently to this effect. The α-face is smooth, while the two CH_3 groups sticking out from the β-face make it more rough. It has been suggested that saturated acyl chains prefer interactions with the α-face, while unsaturated chains should pack better with the β-face [37,38]. Effectively, unsaturated chains have a lower affinity for CHOL than saturated chains, which is further pronounced in the case of polyunsaturation [39].

Considering the high number of molecular components in the membranes of living cells, it is useful to begin with simplified models and proceed towards increasing complexity. After the simplest one-component lipid bilayers, the next step towards lipid raft mixtures are binary mixtures of CHOL with either PC or SM. However, as the data in this review highlights, the understanding of molecular interactions in binary systems does not provide a shortcut toward understanding multi-component bilayers such as ternary mixtures of CHOL, SM and PC.

The discussion below is divided into four parts. Section 2 deals with the properties of one-component SM bilayers and compares them to other bilayers. Section 3 focuses on two-component bilayers, and in particular those where the other component is a sterol. The detailed molecular interactions in a three-component bilayer with dilute concentrations of SM and CHOL are discussed in Section 4, in order to characterize the role of lipid–lipid interactions in the early stages of raft formation. Section 5 finally reviews the large-scale properties of raft-like membranes with large concentrations of SM and CHOL. While the discussion here concentrates on raft-like membranes in the absence of membrane proteins, the coupling of lipid composition on membrane protein activation is discussed through a generic approach for one of the mechanosensitive channels using lateral pressure profiles of a number of different membrane types. Throughout the discussion, we exploit the insight gained through atomistic simulations due to their exceptional added value in complementing experiments on scales of molecular size.

2. Modeling sphingomyelin

2.1. One-component sphingomyelin bilayers

A number of simulations on one-component SM bilayers have been reported in the past few years. Some key results of these simulations are listed in Table 1. The reported experimental values for the area per lipid of SM in the liquid-disordered (l_d) phase vary between 0.47 and 0.55 nm^2 [40,41]. Considering the experimental difficulties in determining the area per lipid and the big scatter among the reported values generally [42], the agreement with simulations is reasonable. Also, the available timescale of the simulations poses a challenge for the comparison. The simulation times of the earlier studies (a few ns) is probably not adequate for complete relaxation of the system and the sampling of conformations to obtain reliable values for the average area per lipid. It is likely that at least several tens of ns should be gathered to sample over multiple autocorrelation times of this value in

Table 1
Key results from simulations of SM bilayers

Lipid	T [K]	A [nm^2]	d_{pp} [nm]	t [ns]	N_{intra}	N_{inter}	N_{water}	Ref
PSM	310	0.515	4.42	5	–	–	–	[50]
PSM	325	0.565	3.60	8	0.81	0.59	–	[49]
PSM	325	0.599	3.85	8	1.04	0.45	–	[49]
PSM	323	0.52	4.34[a]	50	1.08	0.42	5.56	[43]
SSM	323	0.52	4.24[a]	38	0.59	0.41	4.44	[51]
SSM	333	0.48	4.35	20	0.50	0.66	4.13	[52]

The molecules shown are the palmitoyl-SM (PSM) and stearoyl-SM (SSM). In addition to the simulation temperature, T, and the simulation time, t, the columns display the area per lipid, A, the bilayer thickness, d_{pp}, and the estimated numbers of hydrogen bonds, N.
[a] Peak-to-peak distance of electron density plot.

simple membrane systems and even considerably longer times may be needed e.g. in systems with ions [35,43–48].

All publications on SM simulations have extensively concentrated on analyzing hydrogen bond patterns. Even though the abundances and lifetimes of individual bonds are sensitive to the choice of the simulation parameters and the degree of lipid packing [49], the general trends are shared by all studies. Another factor to affect the exact numbers is the definition of hydrogen bond in the analysis. Some studies have inspected radial distribution functions between functional groups [50,51], whereas other studies have utilized geometric cutoffs [43,49,52]. For classical water simulations, also other methods such as energy based cutoffs [53] or more complex cutoffs [54] are commonly used.

The first clear conclusion from the computational studies shown in Table 1 is that the OH-group is the main donor for *intramolecular* hydrogen bonds. The bonds are formed with the phosphate oxygens (mainly with the nearest one), with a very high expectancy. The reported number of intramolecular hydrogen bonds varies from 0.50 [52] up to 1.08 [43] per molecule. Second, the NH-group is the dominating donor for the *intermolecular* hydrogen bonds between lipids. The NH-group binds mainly with the hydroxyl oxygens of other SMs, but to varying extent to carbonyl and other oxygens. The reported number of intermolecular bonds in SM bilayer varies between 0.41 [51] and 0.66 [52] per molecule. Third, water molecules form hydrogen bonds with the phosphate oxygens, but also with other polar groups to some extent. The total number of hydrogen bonds with water varies from 4.13 [52] to 5.56 [43] bonds per lipid. Water creates bridges between lipids. The number of water-bridges in SM bilayer has been estimated to be 0.86 per lipid [52]. In all, a network of both direct and water-mediated hydrogen bonds is formed, resulting in a local clustering of the lipids within the SM bilayer [49]. This has further effects on the properties of the SM bilayer, when compared with PC bilayers (see Section 2.2).

The simulation results on hydrogen bonding have provided support for experimental findings. Previous NMR studies [27,55,56] have proposed both the stable intramolecular bond between the OH-group and the phosphate oxygen, as well as the intermolecular nature of the hydrogen bonds formed by the NH-group. The possibility of water-bridges between sphingomyelins has also been suggested by experiments [27].

2.2. Differences between sphingomyelin and DPPC

To study the effect of hydrogen bonding on the properties of SM bilayer, it is informative to compare the properties of PSM with DPPC.

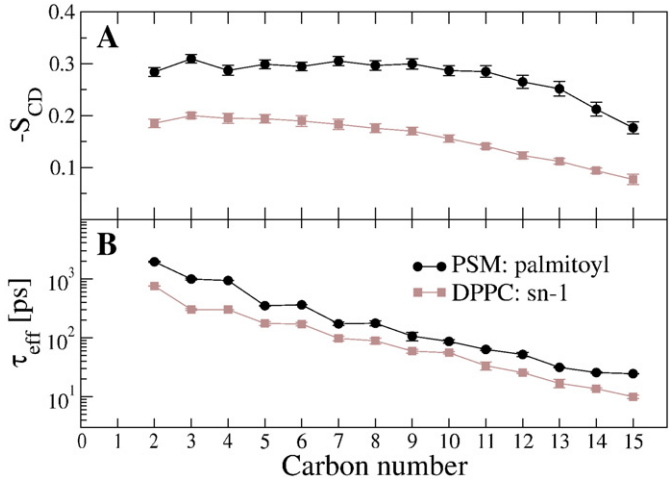

Fig. 2. (A) The deuterium order parameters and (B) the effective rotational autocorrelation times of the CH-vectors of the acyl chains in PSM and DPPC bilayers. The plots are based on [43] (simulations at T=323 K).

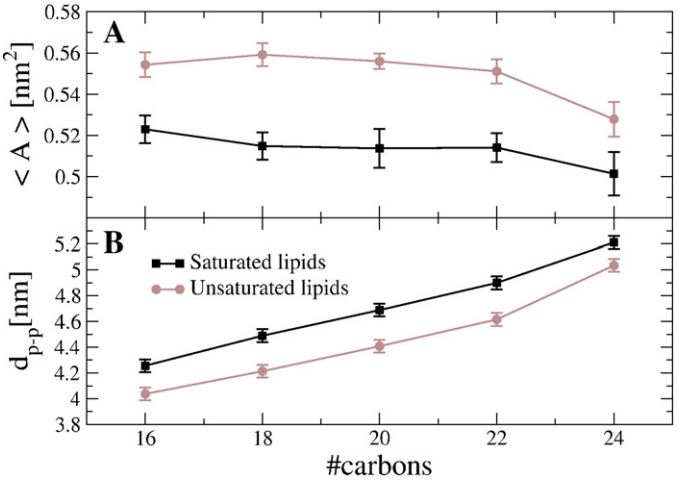

Fig. 3. Average structural quantities of SM bilayers as a function of acyl chain length: (A) area per lipid, and (B) the bilayer thickness. Separate graphs have been drawn for the saturated lipids and for the monounsaturated ones. Figure from [63] (simulations at T=323 K).

Even though the molecular structure of the two lipids is very similar, DPPC lacks the hydrogen bond donors in the interfacial region and can therefore not form direct interlipid hydrogen bonds like PSM.

Perhaps the most evident difference between one-component bilayers of DPPC and PSM are the dimensions of the bilayer. With similar simulation and force field parameters, the area per lipid of PSM, A=(0.52±0.01) nm^2, is significantly smaller than that of DPPC, A=(0.65±0.01) nm^2 [43]. The observed difference is consistent with results from X-ray diffraction [40,41,42]. Since the volumes of the two lipids are very similar, the thickness of PSM bilayer, d=(4.34±0.05) nm, becomes greater than that of DPPC, d=(3.58±0.05) nm [43].

The fact that the PSM bilayer is thicker than DPPC means that the acyl chains are more ordered. This becomes evident from the deuterium order parameter plots in Fig. 2. For comparison, NMR studies suggest significantly higher ordering of the acyl chains [57,58] and of the headgroups [59] in SM than in PC bilayers. Also, in binary SM–PC mixtures, the addition of SM has been shown to increase the overall order of the system [29,60]. It is interesting to note from Fig. 2 that also the rotational dynamics of the acyl chains has significantly slowed down in the SM bilayer, as characterized by the rotational autocorrelation function of the C–H bonds. The rotational dynamics is related to the spin-lattice relaxation times of the NMR experiments [61,62].

Also dynamic features of the lipids, such as the lateral diffusion and overall rotational motions are significantly slowed down in the PSM bilayer when compared with DPPC [43]. For example, the lateral diffusion coefficient is D_T=(0.38±0.03)×10^{-7} cm^2/s for PSM and D_T=(1.27±0.03)×10^{-7} cm^2/s for DPPC. The timescale of the overall rotations of the lipids around their main axis is slowed down from about 1.0 ns (DPPC) to 6.9 ns (PSM).

2.3. Effects of chain length and saturation

Sphingomyelins of biological membranes constitute a variety of molecular species with varying chain length and degree of unsaturation. Only one simulation study has systematically concentrated on the effects of chain length and saturation on the properties of one-component SM bilayers [63]. The following section reviews the most important results from the related study.

Fig. 3 summarizes the dimensions of the simulated SM bilayers in [63]. First, for all chain lengths, mono-unsaturation increases the area per lipid significantly when compared with saturated SM. This means that a single double bond in one of the two chains is likely to alter the overall fluidity of the bilayer, which in turn is reflected in almost all

other properties of the bilayer. The effect of chain length on the area per lipid is much less clear. There seems to be a slight trend of decreasing area with increasing chain length from 16 up to 24 carbons, but the effect is less significant than that caused by unsaturation.

The most prominent effect of chain length is reflected on the bilayer thickness, which increases linearly with chain length. It has been proposed that the match between the hydrophobic length of an integral protein and the hydrophobic thickness of the membrane could be important for the partitioning of the protein into different membrane environments [64,65]. From this point of view, the high variety of chain lengths of SM may be understood as being important for the cells, as they need to adjust the hydrophobic thickness of their membranes and regulate the partitioning of the membrane proteins.

The results in [63] have revealed that the double bond causes a large but local dip in the order parameter profiles of the acyl chains, but has almost negligible effects close to the chain ends. As for the chain dynamics, a local effect in the vicinity of the double bond was also reported. A natural conclusion from this is that the effect of unsaturation is local and that mono-unsaturation most probably increases the area per lipid through local changes in lateral pressure [66].

2.4. Interdigitation

A highly interesting question is the extent of interaction of the opposite monolayers through the bilayer center. This interaction has been suggested to be mediated by the long acyl chains of the lipids, which interdigitate into the opposing monolayer, thereby providing a mechanism for the transfer of information across the bilayer [67,68]. For example, recent fluorescence experiments on supported asymmetric bilayers have provided evidence that ordered domains on the extracellular leaflet are able to induce domains onto the intracellular leaflet [69,70]. Additionally, theoretical considerations have shown that intermonolayer coupling can cause co-localization of the domains if the coupling strength is high enough [71,72]. As SMs typically have long chains and a relatively large chain length disparity, they make likely candidates for interdigitation. For example, results from Raman spectroscopic experiments [73] have suggested two different interdigitated gel-phases (*partial* and *mixed*) for 24:0-SM. Even though usually related to the gel phase, partial interdigitation has been predicted to be important also for the fluid phase [74].

Detailed evidence of interdigitation in SM bilayers was seen in electron density graphs, measured by X-ray diffraction [75]. The density graphs showed a peak in the middle of the bilayer instead of a trough that is typical for lipids with chains of similar length. Recent simulations [63] have been able to reproduce this density peak for SMs (Fig. 4) consistently with the profiles from X-ray diffraction. A more detailed analysis of the simulations has lead to the conclusion that the peak is indeed caused by the increased packing of the ends of the long chains in the middle of the bilayer.

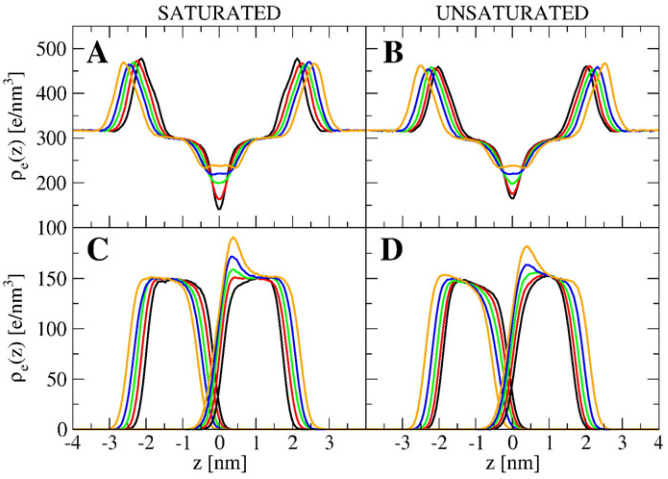

Fig. 4. Electron densities (A, B) across the whole simulated system and (B, C) separately for the sphingosine and the acyl chains of the opposite monolayers. Color coding reflects the acyl chain length of the SM in the simulation: 16 (black), 18 (red), 20 (green), 22 (blue), and 24 (orange). Figure from [63] (simulations at T=323 K).

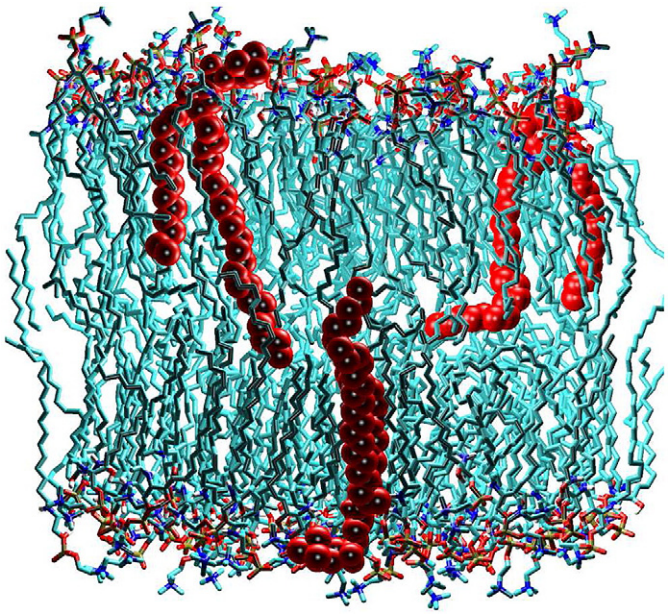

Fig. 5. Snapshot from the simulation of 24:1-SM bilayer. A few molecules have been rendered differently to highlight the different molecular conformations and interdigitation through the bilayer center. The figure is a snapshot from the end of a 50-ns simulation in [63].

Two effects are observed from the two lower panels of Fig. 4: the longer chains reach further towards the opposite monolayer, but on the other hand, there is also a significant contribution from chains that are bent (see Fig. 5 illustrating the two possible conformations). Even though the simulations in [63] have been successful in reproducing the mid-bilayer peak and explaining its origins with the molecular conformations, it remains difficult to quantify the possible biological significance of the observed effect by standard equilibrium simulations. One possibility would be to conduct non-equilibrium simulations in order to measure the interlayer friction for varying systems [76].

3. Modeling sterols

3.1. Different sterols mixed with PC

In order to understand the detailed structure–function relationship of CHOL, one of the most useful means is to compare the effects of CHOL in PC bilayers with other sterols. As an example, Fig. 6 depicts the deuterium order parameters of the acyl chains of DPPC and dioleoyl-PC (DOPC) in binary mixtures with different sterols. The other sterols in the figure are desmosterol and ketosterol, of which desmosterol is particularly interesting since it is cholesterol's direct precursor in its synthetic pathway. Additionally, there is data for an artificially demethylated cholesterol (called DCHOL), see the molecular structures in Fig. 1.

From Fig. 6 it is evident that all sterols are capable of increasing the order of the acyl chains. For unsaturated chains (DOPC), the effect is smaller than for saturated chains (DPPC). Moreover, the differences between sterols in saturated membranes are much larger than in unsaturated membranes. Actually CHOL and desmosterol behave exactly similarly in the DOPC environment, as supported also by experiments [77]. However, none of the sterols in Fig. 6 is better than

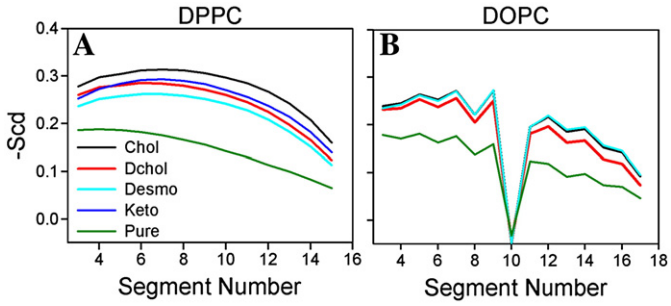

Fig. 6. Deuterium order parameter profiles of the *sn*-1 chain of (A) DPPC and (B) DOPC in pure bilayers and in bilayers containing 20 mol% of different sterols. Image adapted from [95] (simulations at T=323 K).

CHOL in terms of promoting the order of either DPPC or DOPC environment.

A number of studies have compared the properties of CHOL with other sterols, utilizing various research methods such as NMR [77–80], a combination of experiments [77,81], and computer simulations [82–88]. From these studies, it seems that none of the precursors of CHOL in the synthetic pathway (e.g. lanosterol, desmosterol, 7-dehydrocholesterol) are as effective in ordering acyl chains as CHOL [78,79,82–85]. Neither have artificial, completely or partly demethylated and smooth sterols been able to beat the ordering capacity of CHOL [87,88], let alone any of the plant sterols studied so far [80,81].

Some additional remarks on the recent work by Pöyry et al. [88] are appropriate here. They studied the ordering capability of a number of demethylated (synthetic) sterols where the number and positions of methyl groups on the rough side of CHOL were varied systematically. They found that there is one methyl group that is far more important than the others: the C18 group which resides between the third and fourth ring of cholesterol on the rough β-side. The simulation data indicated that C18 is crucial for the proper orientation of the sterol, which in turn correlates with the sterol's capability to order nearby lipid chains [88,89].

Perhaps surprisingly, ergosterol, which is common in lower eukaryotes (fungi, yeast), increases the order of saturated acyl chains more effectively than CHOL [78,79,82,83,86]. It has been proposed that the main reason for this are the additional methyl group and the double bond of the sidechain of ergosterol, which restrict the conformational mobility and lead to more effective packing [86]. However, despite the above elaborate studies, it is evident that additional considerations are needed for complete understanding of the structure–function relationship of the many different sterols, and especially cholesterol.

3.2. Cholesterol mixed with sphingomyelin

A number of simulation studies on binary mixtures of SM and CHOL have been published recently. Cholesterol has been shown to increase the order of the acyl chains of SM, leading to a thicker and more packed bilayer [52,90–92]. In a detailed comparison, SM–CHOL bilayers have been reported to be more packed than PC–CHOL bilayers with a structurally corresponding PC [52,90]. This could be explained either by preferential interaction between SM and CHOL, or by the interlipid interactions between SM molecules. The latter causes also one-component SM bilayers to be more ordered than PC bilayers [43]. In some cases, the addition of CHOL into one-component bilayers actually increases the relative order of PC bilayers more than that of SM bilayers [90].

All studies of binary SM–CHOL mixtures have reported significant hydrogen bonding between these two molecules. The hydroxyl group of CHOL can act both as a donor and an acceptor, making bonds mainly with the carbonyl oxygen, the two phosphate ester oxygens, as well as the amide and hydroxyl groups of SM molecules [52,90]. The number

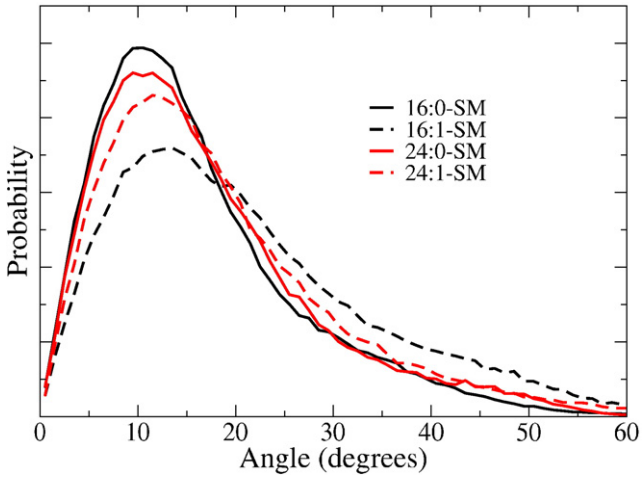

Fig. 7. Cholesterol tilt distributions in binary SM–CHOL bilayers, where CHOL concentration is 20 mol%. Here, the tilt is defined as the angle between the vector along the steroid moiety of CHOL and the bilayer normal. Results of four systems have been shown with different molecular species of SM (unpublished data, T=323 K).

of hydrogen bonds between SM and CHOL is much higher than the number between PC and CHOL [52] or between PS and CHOL [92]. This leads to a more robust hydrogen bonding network in a SM–CHOL bilayer than in other binary mixtures [92].

In a similar way as unsaturation increases the fluidity of one-component SM bilayers, it increases the fluidity of binary SM–CHOL bilayers. For example, changing the stearoyl chain of SM to an oleoyl chain increased the area of a binary SM–CHOL mixture (34 mol% CHOL) from 39.4 nm^2 to 41.2 nm^2 [90]. In our simulations of binary SM–CHOL bilayers with 20 mol% CHOL (unpublished data, parameters as in [63,93], but the *cis*-double bond as in [94], T=323 K, simulation time 100 ns) we have seen that a change from 16:0 chain to 16:1 chain increases the area per molecule from 0.44 nm^2 to 0.49 nm^2. For long chains, the change is less significant, though: a change from 24:0 chain to 24:1 chain resulted in an increase from 0.43 nm^2 to 0.46 nm^2.

As no previous simulation studies exist in the literature for binary mixtures of long-chained SMs with CHOL, it is interesting to view the details of the simulation mentioned above. Fig. 7 shows the tilt of cholesterol ring with respect to bilayer normal in four systems with different SM. As discussed in Section 3.1 and in [95], the tilt of a sterol is a measure of the overall order of the bilayer. Fig. 7 reveals that the tilt of CHOL increases with mono-unsaturation and that the effect is more pronounced in the case of 16:1-SM than 24:1-SM. The effect of

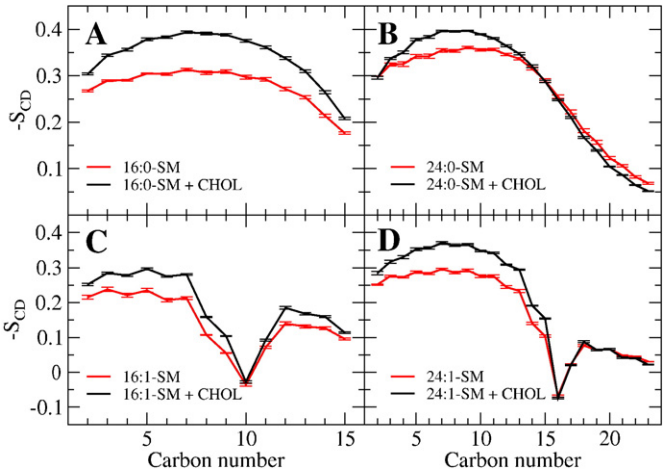

Fig. 8. Each of the four panels display the deuterium order parameter profiles of the hydrocarbon chains of SM in two different bilayers: a one-component SM bilayer (red curves) and a binary SM–CHOL bilayer (black curves). (unpublished data, T=323 K).

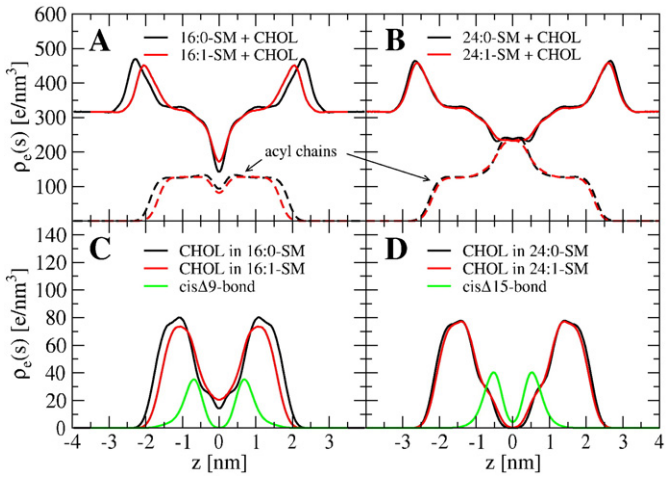

Fig. 9. Electron densities (A, B) of the whole simulated system (solid lines) and of the acyl chains (dashed lines), together with (C, D) the densities of CHOL and the two *cis*-double bonds. All figures represent simulations of binary SM–CHOL systems (unpublished data, T=323 K).

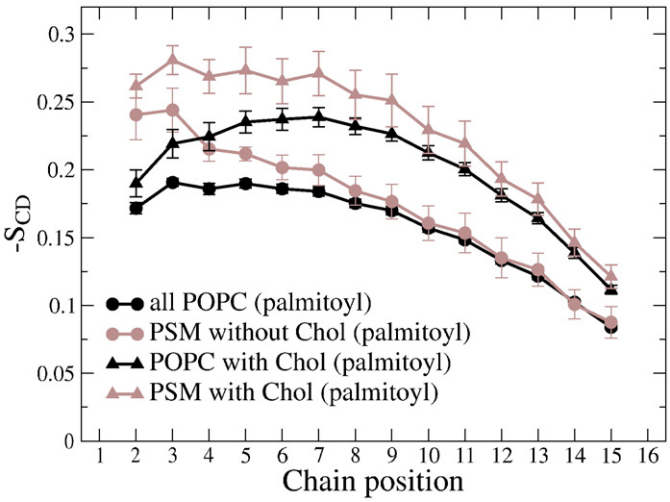

Fig. 10. The deuterium order parameters of the palmitoyl chains of PSM and POPC, plotted separately for those lipids that are either neighbors or non-neighbors of CHOL. Plot redrawn from the data of [89] (simulations at T=310 K).

chain length is less clear: for saturated chains, the system with 24:0-SM seems to have slightly more tilted CHOL molecules than the system with 16:0-SM. For unsaturated chains the effect is opposite.

More detailed insight on ordering is provided by the deuterium order parameter profiles in Fig. 8, which are plotted for one-component SM bilayers and binary SM–CHOL bilayers separately. It is clear that CHOL increases the order of all carbons of the hydrocarbon chains of 16:0-SM and 16:1-SM (except for the double bond position). However, for 24:0-SM and 24:1-SM the effect is limited to carbons C3–C13 and C2–C15, respectively. This means that the effect of CHOL is negligible close to the ends of the long chains. Another finding in Fig. 8 is the higher acyl chain ordering in the long-chained SMs with respect to short chained SMs.

A partial explanation to the above observed effects can be obtained from the density plots in Fig. 9. First, the densities of CHOL and the *cis*-double bond have significant overlap in the 16:1-SM bilayer but not in the 24:1-SM bilayer. This means that the double bond of 16:1-SM is likely to disturb the tilt of CHOL as was seen in Fig. 7. Second, the ends of the 24:0 and 24:1 chains are not affected by CHOL, because the contact between them is unlikely: the high density region of the chains at z=0 in Fig. 9B corresponds to zero density of CHOL at the same location. This is not the case for 16:0-SM and 16:1-SM, whose chains overlap with CHOL over the whole length. The third interesting point in Fig. 9 is the significant interdigitation through the bilayer center in the 24:0-SM and 24:1-SM bilayers, similarly as in the one-component SM bilayers in Fig. 4. The plots in Fig. 9 reveal that the interdigitation in these bilayers is entirely conducted by the long chains of SM and that e.g. CHOL does not take part in interdigitation.

4. Modeling a dilute raft mixture

4.1. CHOL and SM in a matrix of POPC

Even though some aspects of the lipid interactions may be understood from simulations of two-component mixtures, understanding the nature of the interactions that are important for raft formation requires detailed studies of multi-component bilayers. Only a few published simulation studies have extensively addressed the lipid interactions in ternary mixtures of PC, SM, and CHOL. Starting from random mixtures with equal molar fractions, the molecular radial distribution functions have revealed qualitative differences between SM–CHOL and PC–CHOL interactions [37,93]. However, no significant differences in the coordination numbers, nor clear phase separations have been found in the timescales accessible for atom-scale molecular dynamics simulations. Another aspect is to study the interactions in a dilute mixture of SM and CHOL with excess matrix of unsaturated PCs [89]. This approach addresses the nature of interactions in a more fluid-like environment.

First, to understand the capacity of CHOL to order the acyl chains of neighboring lipids, let us examine Fig. 10. The figure shows the deuterium order parameters of the saturated palmitoyl chains of both PSM and POPC in two situations: when the lipid has a CHOL neighbor, and when it has none (i.e. it has only POPC neighbors). The figure reveals clearly that, throughout the chain length, CHOL increases the order of the acyl chain of both types of neighboring lipids. This conclusion is in agreement with a previous molecular dynamics simulation study, which showed that CHOL has a tendency to order the neighboring acyl chains within a radius of a few nanometers [39].

Another clear conclusion from Fig. 10 is that CHOL increases the ordering of PSM more than that of POPC. On average, the order parameter in POPC changes by 0.041 but in PSM by 0.066. This is an indication of the different nature of the PSM–CHOL interaction when compared to the POPC–CHOL interaction. Here one should note that

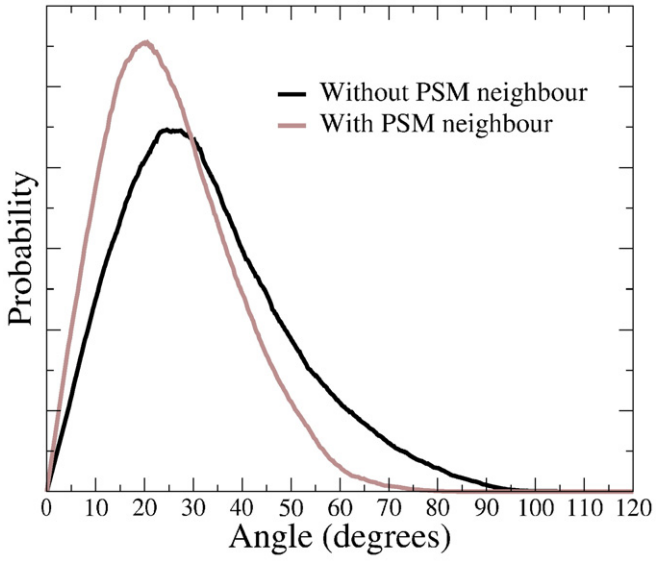

Fig. 11. The angular distribution of the ring structure of CHOL with respect to the bilayer normal, plotted separately for those CHOL molecules that have a PSM neighbor and those that do not. Figure adapted from [89] (simulations at T=310 K).

the difference must be due to local lipid–lipid interactions, because the overall membrane environment, dictated by the excess POPC matrix, may be assumed to be similar for each of the separate CHOL molecules in the system.

An additional aspect of the order of CHOL may be realized from Fig. 11, which presents the tilt of CHOL molecules with respect to the bilayer normal in two different situations: when surrounded only by POPC molecules, and second, when one of the neighbors is PSM. The graphs reveal that having a PSM neighbor induces a significantly less tilted orientation of CHOL with respect to the bilayer normal. Clearly, the close neighborhood of PSM increases the order of CHOL — another indication of a specific interaction between these molecules.

The high ordering capacity of CHOL is usually related to the attractive van der Waals interactions between the hydrophobic parts of CHOL and the acyl chains. For example, MD simulations have shown that saturated chains favor the smooth α-face of CHOL instead of the rougher β-face [37,38]. The results by Aittoniemi et al. [95] support this idea. The saturated chains of POPC and PSM are on average more ordered when next to the α-face of CHOL than the β-face, whereas the unsaturated chain of POPC shows no such difference. The differential ordering of the acyl chains on the two sides of CHOL possibly also explains the observed preference of PSM for the α-face.

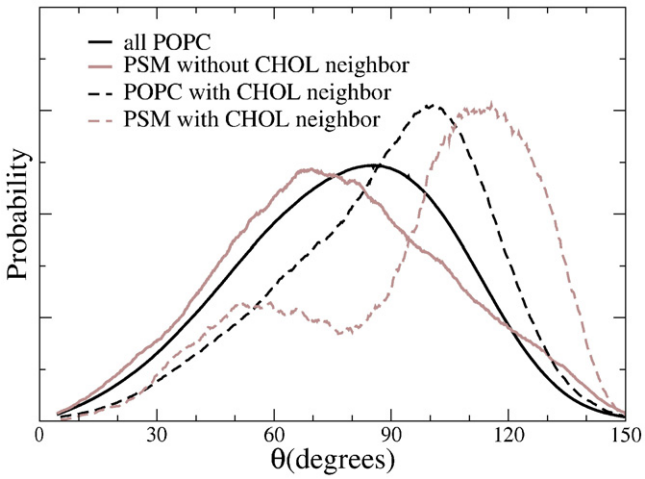

Fig. 13. Angular distribution of the headgroup P–N vector with respect to the bilayer normal. Plotted separately for those PSM or POPC molecules that are either nearest neighbors of CHOL and for those that are not. Figure adapted from [89] (simulations at T=310 K).

4.2. Hydrogen bonds and headgroup interactions

The hydrogen bonding characteristics between POPC, PSM and CHOL molecules in the simulations by Aittoniemi et al. have been summarized in detail in [89]. Perhaps the most notable effect is the nearly complete lack of direct hydrogen bonds between CHOL and PSM. Previous simulation studies of ternary PC–SM–CHOL mixtures [37,96] have not reported any direct hydrogen bonds between SM and CHOL either. Considering the much higher number of direct bonds between other molecular pairs such as CHOL–POPC and PSM–POPC, it seems evident that direct hydrogen bonding cannot be the principal interaction that would lead to molecular attraction between PSM and CHOL within a PC matrix, at least at low CHOL/PSM concentrations. On the other hand, the hydrogen bonding patterns of CHOL and SM seem to be altered when they are next to each other, even though no direct hydrogen bonding is observed. The bonds of CHOL with water are diminished when it has a PSM neighbor, and on the other hand, the number of intramolecular bonds of a PSM is increased when it has a CHOL neighbor.

In addition to hydrogen bonds, other electrostatic interactions play a role in lipid–lipid interactions. For example, the headgroups of both PC and SM consist of a negatively charged phosphate and a positively charged choline group. The interactions between a set of headgroups are understood in terms of a dipole–dipole interaction, which is either attractive or repulsive depending on the relative orientations of the dipoles. Even though the headgroup is incapable of forming hydrogen bonds, a net attractive electrostatic interaction is possible with the OH-group of CHOL and the positively charged choline. A snapshot showing the typical conformation that involves this interaction is in Fig. 12.

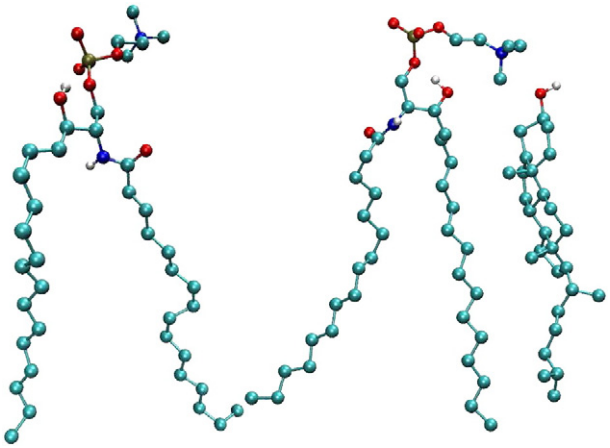

Fig. 12. Snapshots representing typical PSM orientations, for a PSM without CHOL neighbor (left) and a PSM with CHOL neighbor (right). Figure adapted from [89].

The simulation study by Aittoniemi et al. [89] showed that even though PSM seems "reluctant" to form direct hydrogen bonds with CHOL, the charge-pairs between its headgroup and CHOL are relatively much more abundant than those between POPC and CHOL. The distributions of the headgroup orientations with respect to bilayer normal in the two cases are plotted in Fig. 13. Without a CHOL neighbor, the headgroup of POPC is tilted somewhat more towards the bilayer center than the headgroup of PSM. The neighborhood of CHOL makes an interesting difference, however. While the tilt of POPC's headgroup changes only slightly, the headgroup of PSM becomes more tilted towards the bilayer center than the one of POPC. At the same time, the distribution of the headgroup angles becomes bimodal for PSM. An analysis of the hydrogen bonding patterns hints that the intramolecular hydrogen bonding of PSM might help in stabilizing the bending of the PSM's headgroup downwards and thus further the charge-pair interaction between PSM and CHOL. The idea is illustrated in the two snapshots of Fig. 12.

Another related interaction is the so-called umbrella effect [97], which is probably enhanced by the charge-pairing interaction. The idea of the umbrella effect is based on the fact that CHOL is largely hydrophobic and benefits when shielded from water by other headgroups. A more detailed analysis in [89] revealed that the hydrophobic parts of CHOL have less overlap with water when charge-paired with PSM than when charge-paired with POPC. Based on this observation, it was proposed that the combination of charge-pairing and hydrophobic effects could be more important for PSM–CHOL interaction than direct hydrogen bonding.

However, the fact is that the situation is complex with many competing effects taking place simultaneously, which makes it difficult to estimate the relative strengths of the different effects even in this relatively simple three-lipid composition. The issue remains to be solved more accurately with detailed free-energy calculations. One recent study has pioneered into this direction [98], calculating the free energy of transfer of CHOL from POPC to SM environment. The obtained value of 5–10 kJ/mol reflects a small

Table 2
Average structural and thermodynamic properties of three membrane systems simulated in [93], i.e. two raft-like membranes (POPC:PSM:CHOL=1:1:1 and 2:1:1) and one non-raft membrane (POPC:PSM:CHOL=62:1:1)

POPC:PSM:CHOL	1:1:1	2:1:1	62:1:1
A [nm^2]	0.41±0.01	0.44±0.01	0.66±0.01
d [nm]	4.40±0.05	4.29±0.05	3.53±0.05
$-S_{CD}$ (5–7)	0.41	0.36	0.18
K_A [10^{-3} N/m]	2700±700	1000±400	200±100
k_c [10^{-20} J]	10±2	7±2	6±2
D_{popc} [10^{-7} cm^2/s]	0.037±0.002	0.08±0.02	0.67±0.06
D_{psm} [10^{-7} cm^2/s]	0.036±0.002	0.07±0.02	0.8±0.2
D_{chol} [10^{-7} cm^2/s]	0.038±0.002	0.08±0.02	0.5±0.2

The results indicate: average area per lipid (A), bilayer thickness (d), average deuterium order parameter (S_{CD}) of acyl chain carbons 5–7, area compressibility modulus (K_A), bending rigidity modulus (k_c), and lateral diffusion coefficients (D). All results are at T=310 K.

preference of CHOL for the SM environment. From the point of view of the study by Aittoniemi et al. [89], it would be rather informative to calculate the free energy of transfer of CHOL from pure POPC environment to an environment with one SM neighbor. This should be able to give information about the leading contributions to the free energy.

5. Modeling lipid raft mixtures

5.1. Raft-like vs. non-raft membranes

Average properties of three simulated membrane compositions from [93] are summarized in Table 2. The first observation is the strongly condensed nature of the two raft-like membranes (POPC:PSM:CHOL=1:1:1 and 2:1:1) when compared to the non-raft like membrane (POPC:PSM:CHOL=62:1:1) discussed in the previous section. The decreased area per lipid, together with the increased bilayer thickness and order parameter values indicate that acyl chains in the raft-like membranes are much more highly packed than in the non-raft membrane. When looking at the values for area compressibility, K_A, and bending rigidity, k_c, it is evident that the raft-like membranes are characterized by a much more rigid nature than the more fluid non-raft membrane. The lateral diffusion coefficients, D, reveal about an order of magnitude slower dynamics in raft-like membranes when compared to the non-raft bilayer.

Recent experiments give further support for the results represented in Table 2. First, an AFM study reported a thickness variation of 0.6–0.9 nm in a bilayer that displayed a phase coexistence of the l_d and l_o domains [99]. Second, an X-ray diffraction study displayed a thickness difference of 0.9 nm between detergent resistant (raft) and soluble (non-raft) membranes [100]. These studies are in agreement with the thickness differences of the simulated bilayers. Another point of comparison is a pulsed-field NMR study [101], which reported two populations of diffusion coefficients in DOPC–SM–CHOL mixtures with 10–30 mol% CHOL at 300 K, one corresponding to the l_d phase ($D\approx 1\times10^{-7}$ cm^2/s) and the other to the l_o phase ($D\approx 1\times10^{-8}$ cm^2/s). The agreement of these experimental results with the values in Table 2 support the idea that the simulated raft-like membranes are representatives of the environment within a l_o domain, and the non-raft simulation that of the l_d domain.

The bilayer dimensions, A and d, of the non-raft bilayer are in agreement with a previous X-ray diffraction study [102] and an MD simulation [103] on pure POPC bilayers in the l_d phase. Also, the area compressibility modulus, K_A, and the bending rigidity, k_c are in line with previous computational studies [104] and experimental micropipette studies [105,106] of pure PC bilayers, reporting values of K_A=140–300×10^{-3} N/m and k_c=4–9×10^{-20} J.

The two simulations of raft-like membranes may be compared with binary PC–CHOL systems with similar CHOL concentrations. Comparison with previous simulation studies [34,35] shows that the values for A in Table 2 for raft-like bilayers are 0.1 to 0.4 nm^2 lower than expected for binary PC-CHOL systems with similar CHOL concentrations. Also, the differences in K_A values for raft-like membranes are higher than reported earlier by simulations [34] or micropipette experiments [107], predicting maximally 5–7 fold increase in the K_A values upon addition of CHOL into PC bilayers. Particularly interesting is the micropipette manipulation study of vesicles [108], which reported a much higher value of K_A=1718×10^{-3} N/m for a SM–CHOL bilayer than the value of K_A=781×10^{-3} N/m

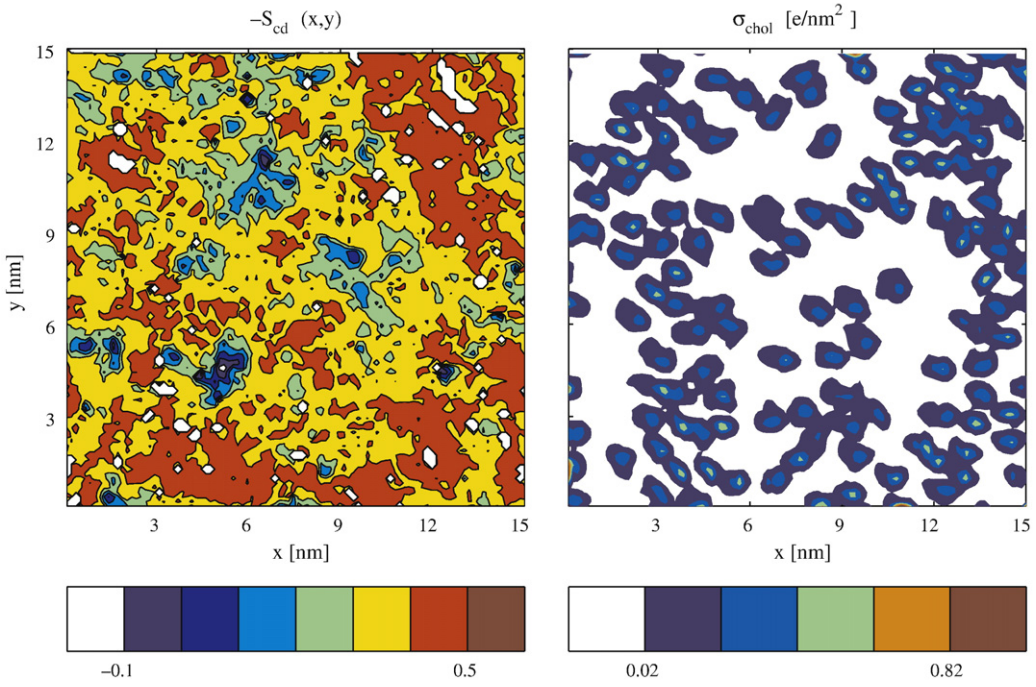

Fig. 14. The deuterium order parameters of selected carbons (C5–C7) in POPC and PSM chains (left) and the CHOL density (right), binned in the xy-plane and averaged over 10 ns. The plot is for one of the two leaflets in the system with POPC:PSM:CHOL=2:1:1. Figure adapted from [93] (simulations at T=310 K).

for a PC-CHOL bilayer, both with 50 mol% CHOL. Concluding, the above values suggest an additional role of PSM in ordering and rigidifying the bilayer. This is possibly related to the additional intermolecular hydrogen bonds induced by PSM.

5.2. Lateral heterogeneity

Simulations in [93] have revealed two types of nano-scale lateral heterogeneity in the three-component mixtures. The first type was prominent in the raft-like bilayers and seems to be related to the tendency of CHOL to order the neighboring acyl chains. Fig. 14 shows the average order parameters of acyl chains for one of the raft-like membranes, plotted over the *xy*-plane and averaged over 10 ns. Comparison with the neighboring plot for lateral density of CHOL over the same time interval shows a clear correlation. The areas with higher lateral density of CHOL correspond to higher acyl chain order, whereas areas of depleted CHOL display higher disorder.

The other type of lateral heterogeneity was observed in the non-raft bilayer, as displayed in Fig. 15. Here, the small concentration of CHOL seems insufficient to fully account for the observed large-scale lateral heterogeneity in chain order parameters. Instead, the regions of higher order seem to be related with the thickness fluctuations of the membrane. As can be seen from Fig. 15, the more ordered regions are correlated with the thicker regions of the membrane and the less ordered regions with thinner regions. The idea is supported by the fact that the large-scale peristaltic modes are much more pronounced in the non-raft membrane than in the raft-like membranes, as indicated by [93]. Recent studies for one-component bilayers also support the view of a correlation between local density and membrane order [109].

The above conclusions on lateral heterogeneity may be debated because of the slow dynamics and the inadequate conformational sampling in the raft simulations. However, while the two raft-like simulations were started from different initial configurations, they lead to similar conclusions. Furthermore, a characterization of the pair distribution functions between the lipids in time displayed significant changes and convergence over time, which is an indication of relaxation of the structure at small length scales.

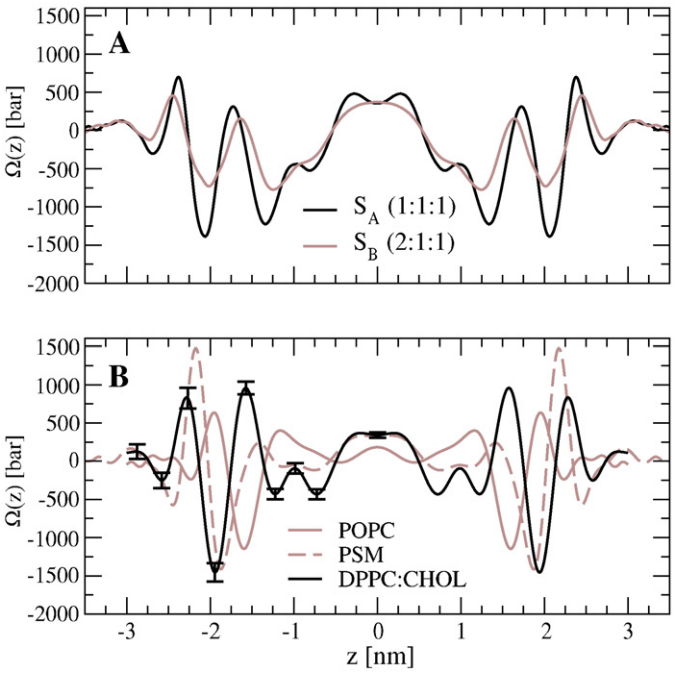

Fig. 16. Lateral pressure profiles of (A) raft-like membranes, together with (B) pure POPC/PSM systems and a binary DPPC–CHOL system. The center of the membrane is at $z=0$ in each plot. Figure adapted from [93].

5.3. Lateral pressure profiles and membrane proteins

Membranes are characterized by a lateral pressure profile, which essentially describes the force (pressure) exerted by the membrane on a particle embedded inside a membrane. Lateral pressure profiles have been suggested to influence the structure and dynamics of membrane proteins [63,110,111]. Additionally, the changes in lateral pressure profile, $\Omega(z)$, are probably related to the mechanism of general anesthetics [112,113] and consequently relate membranes to a number of cellular functions.

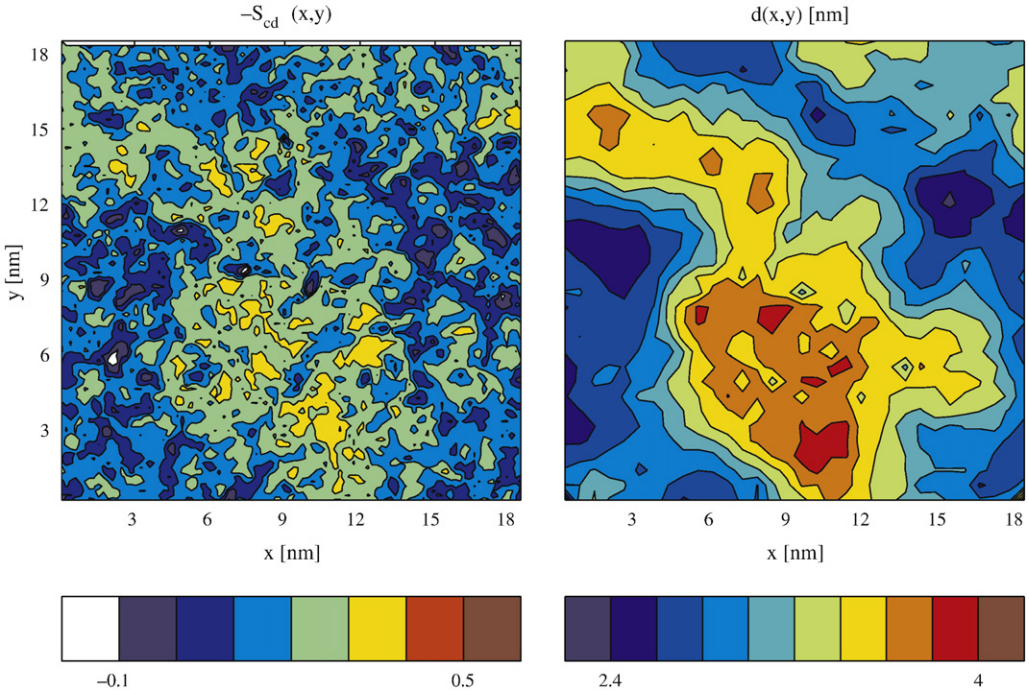

Fig. 15. The deuterium order parameters of selected carbons (C5–C7) in POPC and PSM chains (left) and the average thickness of the bilayer (right), binned in the *xy*-plane and averaged over 10 ns. The plot is for one of the two leaflets in the system with POPC:PSMCHOL=62:1:1. Figure adapted from [93]. (simulations at $T=310$ K).

Fig. 16 shows the lateral pressure profiles of different kinds of lipid bilayers calculated from MD simulations of raft-like and non-raft membranes [93]. It is interesting to note that even though the integral over $\Omega(z)$ must be zero due to the boundary condition of zero surface tension, the local pressures within the bilayer are in the order of 1000 bar in magnitude. The origins and the nature of the different peaks in $\Omega(z)$ have been discussed in recent literature and e.g. the contributions from different components of the simulation force field have been calculated separately [114–117].

The pressure profiles for different systems, as shown in Fig. 16 are qualitatively different. In particular, membranes that contain CHOL display a higher number of peaks when compared to single-component bilayers. Also, the raft-like membranes display further characteristics due to the simultaneous presence of SM and CHOL. Rather than conducting a detailed analysis of all peaks and their origins, the following discussion concentrates on more general aspects about the possible biological implications of lateral pressure profiles.

To estimate the effect of pressure profile on membrane proteins one can follow the approach introduced by Cantor [110] and later used by Gullingsrud et al. [111]. The idea is to calculate the work ΔW done against the lateral pressure profile when altering the shape of the membrane cavity occupied by the protein as it changes its conformation from the closed to an open state. Assuming that the cross-sectional area of the protein changes by $\Delta A(z)$, as a function of distance from membrane center z, the work can be written as:

$$\Delta W = \int dz\, \Omega(z) \Delta A(z). \quad (1)$$

The ion channel MscL provides a good example case, because its conformation changes anisotropically between cylindrical (closed) and cone (open) shapes [118], see Fig. 17 for schematic illustration. Both conformations can roughly be described by the cross-sectional area of a truncated cone $A(z)=\pi(R+sz)^2$. The slope, s, and the radius, R, are fitted to the experimental structure of MscL and are identical to those used by Gullingsrud et al. [111]. Using this simple scheme, one can calculate the work done against the lateral pressure profile in opening the channel.

The integration over the lateral pressure profiles in Fig. 16 results in $\Delta W=(11\pm2)\ k_BT$ and $(4\pm1)\ k_BT$ for the two raft-like membranes, with POPC:PSM:CHOL=1:1:1 and 2:1:1 in respective order. These are significantly higher than the values found for the pure POPC bilayer $(1.9\pm0.2)\ k_BT$, the pure PSM bilayer $(1.0\pm0.6)\ k_BT$, or the binary DPPC–CHOL bilayer $(1.0\pm0.4)\ k_BT$. The numbers above suggest that the equilibrium probability of MscL to be in open state is significantly altered by the pressure profile and is higher in the raft-like membranes than in any of the (non-raft) reference membranes. As the free energy difference between the open and closed states of MscL has been estimated to be about 20–50 k_BT [119,111], the pressure profile contributes a significant fraction of this total free energy difference.

This supports the view that protein–lipid interactions do matter, and lipids indeed are involved in the activation of membrane proteins.

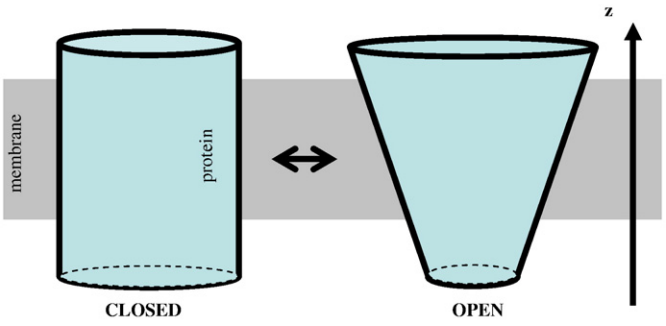

Fig. 17. Schematic illustration of the two conformations of the membrane protein MscL embedded in a lipid bilayer.

The simplified example above suggests that lateral pressure profiles are able to influence protein activation through changes in membrane elastic coefficients. Similar findings have been made in experiments as well: it has been found that some membrane protein types are sensitive to the elastic properties of the membrane [120,121]. Bearing in mind that essentially all elastic coefficients of membranes can be derived from the lateral pressure profile [122], it is no wonder that the lateral pressure profile plays an important role in protein activation.

6. Summary

The complexity of biological membranes and the large variety of involved length and time scales calls for a multitude of research approaches, including molecular dynamics simulations in atomic detail. This review has concentrated on simulation studies of 1) one-component bilayers consisting of either PC or SM, 2) binary mixtures of SM or PC with sterols, and 3) ternary mixtures of SM, PC, and CHOL.

Simulation results for one-component SM bilayers have shown that the intra- and intermolecular hydrogen bonding leads to significant differences in the bilayer properties when compared with PC. For example, packing of the lipids and the ordering of the acyl chains are more pronounced in the SM bilayers. Also, the higher degree of saturation and the long nature of the acyl chains in SM has been found to alter the structure and dynamics of the bilayers. In particular, the long chains of both saturated and monounsaturated SMs have been found to interdigitate through the bilayer center.

Studies on binary mixtures of PC and sterols have revealed that CHOL is more effective in increasing the order of saturated acyl chains than most other sterols, and that it also increases the order of monounsaturated chains. Additionally, binary SM–CHOL mixtures have reported to be more ordered than corresponding PC–CHOL mixtures, which is a result of different molecular interactions (either hetero- or homo-molecular) in these systems. Significant numbers of both direct and water-mediated hydrogen bonds have been reported in binary SM–CHOL bilayers. In fact, the number of hydrogen bonds has been reported to be much higher than in binary PC–CHOL bilayers.

New simulation results on binary SM–CHOL bilayers were discussed in this report, comparing properties of bilayers with long and short chained SMs. The simulations revealed significant interdigitation through the bilayer center in systems with 24:0-SM and 24:1-SM, in a similar fashion as for one-component SMs. It was found that CHOL molecules do not reach the mid-bilayer region in these mixtures, but they do in mixtures with 16:0-SM and 16:1-SM. The tilt of CHOL was found to be disturbed significantly more by the *cis*Δ9-double bond of 16:1-SM than by the *cis*Δ15 of 24:1-SM. The reason for this is that the double bond of the 16:1 chain has more contact with CHOL than the one in the 24:1 chain.

In simulations of ternary mixtures of SM, PC, and CHOL, no direct hydrogen bonding has been seen between SM and CHOL. Rather, the difference in molecular interaction has been suggested to be related to the interactions between CHOL and water. Simulations of raft-like membranes have lead to more rigid, ordered and packed bilayers than non-raft like membranes, the former also characterized by slower dynamics overall. The different properties of the two membrane environments have been suggested to have significant implications for membrane proteins, in particular through differences in the lateral pressure profiles of the membrane.

Ideas for further studies are manyfold. First, simulations of single-component bilayers should be continued to further the understanding of the characteristics of different lipid species, and to develop ways to better combine simulations with experiments. Work on multi-component systems should be continued as well in order to gain more insight into the molecular interactions between different lipid species. In particular, this would help in developing new coarse-grained models for the different lipid species, which in turn would allow for studies of many slow or large-scale phenomena. Recently,

several studies into this direction have been published. For example, coarse-grained models have facilitated studies of CHOL containing mixtures on very large length- and timescales, either utilizing the Inverse Monte Carlo technique [123,124] or another mean field technique [125,126]. These studies have been able to make predictions e.g. on the concentration dependence and lifetimes of the domains. The somewhat less coarse-grained MARTINI model by Marrink et al. [127,128] has been widely used recently for lipid simulations. For example, domain formation in a binary lipid mixture [129], formation and the melting of the gel phase [130], the flip-flops of CHOL in polyunsaturated membrane [128], or the pressure–area behaviour of lipid monolayers [131] have been studied by using this model. It seems evident that the MARTINI model will become popular in large-scale studies of a broad range of membrane phenomena.

Another aspect for the future is to develop new setups that more realistically describe real biological membranes. For example, simulations on asymmetric bilayers [132,47], or bilayers involving glycolipids [133,134] are rare but doable. Further, the task of simulating full transmembrane proteins in different lipid environments would provide more detailed insights on the features of lipid–protein interactions. The task is difficult, but possible in the near future. Finally, there is reason to keep in mind that cells are in constant motion under non-equilibrium conditions, while most of the simulations are conducted in equilibrium. There is definitely plenty of room for the development of non-equilibrium techniques for the modeling of membrane systems under realistic conditions, including their non-equilibrium nature.

Acknowledgments

This work has, in part, been supported by the Academy of Finland grants and the Academy of Finland Center of Excellence Program, the Jenny and Antti Wihuri Foundation, and the Finnish Academy of Science and Letters. We acknowledge the Finnish IT Center for Science and the HorseShoe (DCSC) supercluster computing facility at the University of Southern Denmark for computer resources.

References

[1] G. van Meer, Cellular lipidomics, EMBO J. 24 (2005) 3159–3165.
[2] E. Sackmann, Biological membranes architecture and function, in: R. Lipowsky, E. Sackmann (Eds.), Structure and Dynamics of Membranes: From Cells to Vesicles, Elsevier, Amsterdam, 1995, pp. 1–65.
[3] S.J. Singer, G.L. Nicolson, The fluid mosaic model of the structure of cell membranes, Science 175 (1972) 720–731.
[4] E. Oldfield, D. Chapman, Dynamics of lipids in membranes: heterogeneity and the role of cholesterol, FEBS Lett. 23 (1972) 285–297.
[5] E.J. Shimshick, H.M. McConnell, Lateral phase separation in phospholipid membranes, Biochemistry 12 (1973) 2351–2360.
[6] K. Simons, E. Ikonen, Functional rafts in cell membranes, Nature 387 (1997) 569–572.
[7] M. Edidin, The state of lipid rafts: from model membranes to cells, Annu. Rev. Biophys. Biomol. Struct. 32 (2003) 257–283.
[8] L.J. Pike, Lipid rafts: heterogeneity on the high seas, Biochem. J. 378 (2004) 281–292.
[9] L.J. Pike, Rafts defined: a report on the keystone symposium on lipid rafts and cell function, J. Lipid Res. 47 (2006) 1597–1598.
[10] T. Hevonoja, M.O. Pentikäinen, M.T. Hyvönen, P.T. Kovanen, M. Ala-Korpela, Structure of low density lipoprotein (LDL) particles: basis for understanding molecular changes in modified LDL, Biochim. Biophys. Acta 1488 (2000) 189–210.
[11] G.W. Feigenson, Phase boundaries and biological membranes, Annu. Rev. Biophys. Biomol. Struct. 36 (2007) 63–77.
[12] R. Varma, S. Mayor, GPI-anchored proteins are organized in submicron domains at the cell surface, Nature 394 (1998) 798–801.
[13] K. Cottingham, Do you believe in lipid rafts? Anal. Chem. 76 (2004) 403–406.
[14] K. Simons, W.L.C. Vaz, Model systems, lipid rafts, and cell membranes, Annu. Rev. Biophys. Biomol. Struct. 33 (2004) 269–295.
[15] K. Gaus, E. Gratton, E.P.W. Kable, A.S. Jones, I. Gelissen, L. Kritharides, W. Jessup, Visualizing lipid structure and raft domains in living cells with two-photon microscopy, Proc. Natl. Acad. Sci. U. S. A. 100 (2003) 15554–15559.
[16] R.E. Brown, Sphingolipid organization in biomembranes: what physical studies of model membranes reveal, J. Cell. Sci. 111 (1998) 1–9.
[17] E. London, How principles of domain formation in model membranes may explain ambiguities concerning lipid raft formation in cells, Biochim. Biophys. Acta 1746 (2005) 203–220.
[18] B. Ramstedt, J.P. Slotte, Membrane properties of sphingomyelins, FEBS Lett. 531 (2002) 33–37.
[19] J.M. Holopainen, A.J. Metso, J.P. Mattila, A. Jutila, P.K.J. Kinnunen, Evidence for the lack of a specific interaction between cholesterol and sphingomyelin, Biophys. J. 86 (2004) 1510–1520.
[20] B. Ramstedt, J.P. Slotte, Comparison of the biophysical properties of racemic and D-*erythro*-*N*-acyl sphingomyelins, Biophys. J. 77 (1999) 1498–1506.
[21] Y. Barenholz, T.E. Thompson, Sphingomyelin: biophysical aspects, Chem. Phys. Lipids 102 (1999) 29–34.
[22] B. Ramstedt, J.P. Slotte, Sphingolipids and the formation of sterol-enriched ordered membrane domains, Biochim. Biophys. Acta 1758 (2006) 1945–1956.
[23] R. Koynova, M. Caffrey, Phases and phase transitions of the sphingolipids, Biochim. Biophys. Acta 1255 (1995) 213–236.
[24] L.K. Bar, Y. Barenholz, T.E. Thompson, Effect of sphingomyelin composition on the phase structure of phosphatidylcholine–sphingomyelin bilayers, Biochemistry 36 (1997) 2507–2516.
[25] R. Koynova, M. Caffrey, Phases and phase transitions of the phosphatidylcholines, Biochim. Biophys. Acta 1376 (1998) 91–145.
[26] J.R. Silvius, Role of cholesterol in lipid raft formation: lessons from lipid model systems, Biochim. Biophys. Acta 1610 (2003) 174–183.
[27] C.M. Talbott, I. Vorobyov, D. Borchman, K.G. Taylor, D.B. DuPré, M.C. Yappert, Conformational studies of sphingolipids by NMR spectroscopy. II. Sphingomyelin, Biochim. Biophys. Acta 1467 (2000) 326–337.
[28] M.P. Veiga, J.L.R. Arrondo, F.M. Goni, A. Alonso, D. Marsh, Interaction of cholesterol with sphingomyelin in mixed membranes containing phosphatidylcholine, studied by spin-label ESR and IR spectroscopies. A possible stabilization of gel-phase sphingolipid domains by cholesterol, Biochemistry 40 (2001) 2614–2622.
[29] W. Guo, V. Kurze, T. Huber, N.H. Afdhal, K. Beyer, J.A. Hamilton, A solid-state NMR study of phospholipid–cholesterol interactions: sphingomyelin–cholesterol binary systems, Biophys. J. 83 (2002) 1465–1478.
[30] M. Bloom, E. Evans, O.G. Mouritsen, Physical properties of the fluid lipid-bilayer component of cell membranes: a perspective, Q. Rev. Biophys. 24 (1991) 293–397.
[31] H. Ohvo-Rekilä, B. Ramstedt, P. Leppimäki, J.P. Slotte, Cholesterol interactions with phospholipids in membranes, Prog. Lipid Res. 41 (2002) 66–97.
[32] T. Xiang, Translational diffusion in lipid bilayers: dynamic free-volume theory and molecular dynamics simulation, J. Phys. Chem. B 103 (1999) 385–394.
[33] P. Jedlovszky, M. Mezei, Effect of cholesterol on the properties of phospholipid membranes. 2. Free energy profile of small molecules, J. Phys. Chem. B 107 (2003) 5322–5332.
[34] C. Hofsäss, E. Lindahl, O. Edholm, Molecular dynamics simulations of phospholipid bilayers with cholesterol, Biophys. J. 84 (2003) 2192–2206.
[35] E. Falck, M. Patra, M. Karttunen, M.T. Hyvönen, I. Vattulainen, Lessons of slicing membranes: interplay of packing, free area, and lateral diffusion in phospholipid/cholesterol bilayers, Biophys. J. 87 (2004) 1076–1091.
[36] M. Kupiainen, E. Falck, S. Ollila, P. Niemelä, A.A. Gurtovenko, M.T. Hyvönen, M. Patra, M. Karttunen, I. Vattulainen, Free volume properties of sphingomyelin, DMPC, DPPC, and PLPC bilayers, J. Comput. Theor. Nanosci. 2 (2005) 401–413.
[37] S.A. Pandit, E. Jakobsson, H.L. Scott, Simulation of the early stages of nanodomain formation in mixed bilayers of sphingomyelin, cholesterol, and dioleylphosphatidylcholine, Biophys. J. 87 (2004) 3312–3322.
[38] T. Róg, M. Pasenkiewicz-Gierula, Cholesterol effects on a mixed-chain phosphatidylcholine bilayer: a molecular dynamics simulation study, Biochimie 88 (2006) 449–460.
[39] M.C. Pitman, F. Suits, A.D. MacKerell, S.E. Feller, Molecular-level organization of saturated and polyunsaturated fatty acids in a phosphatidylcholine bilayer containing cholesterol, Biochemistry 43 (2004) 15318–15328.
[40] P.R. Maulik, G.G. Shipley, *N*-palmitoyl sphingomyelin bilayers: structure and interactions with cholesterol and dipalmitoylphosphatidylcholine, Biochemistry 35 (1996) 8025–8034.
[41] X.M. Li, J.M. Smaby, M.M. Momsen, H.L. Brockman, R.E. Brown, Sphingomyelin interfacial behavior: the impact of changing acyl chain composition, Biophys. J. 78 (2000) 1921–1931.
[42] J.F. Nagle, S. Tristram-Nagle, Structure of lipid bilayers, Biochim. Biophys. Acta 1469 (2000) 159–195.
[43] P. Niemelä, M.T. Hyvönen, I. Vattulainen, Structure and dynamics of sphingomyelin bilayer: insight gained through systematic comparison to phosphatidylcholine, Biophys. J. 87 (2004) 2976–2989.
[44] R.A. Böckmann, A. Hac, T. Heimburg, H. Grubmüller, Effect of sodium chloride on a lipid bilayer, Biophys. J. 85 (2003) 1647–1655.
[45] R.A. Böckmann, H. Grubmüller, Multistep binding of divalent cations to phospholipid bilayers: a molecular dynamics study, Angew. Chem., Int. Ed. 43 (2004) 1021–1024.
[46] A.A. Gurtovenko, M. Miettinen, M. Karttunen, I. Vattulainen, Effect of monovalent salt on cationic lipid membranes as revealed by molecular dynamics simulations, J. Phys. Chem. B 109 (2005) 21126–21134.
[47] A.A. Gurtovenko, I. Vattulainen, Membrane potential and electrostatics of phospholipid bilayers with asymmetric transmembrane distribution of anionic lipids, J. Phys. Chem. B 112 (2008) 4629–4634.
[48] C. Anézo, A.H. de Vries, H.D. Höltje, D.P. Tieleman, S.J. Marrink, Methodological issues in lipid bilayer simulations, J. Phys. Chem. B 107 (2003) 9424–9433.

[49] E. Mombelli, R. Morris, W. Taylor, F. Fraternali, Hydrogen-bonding propensities of sphingomyelin in solution and in a bilayer assembly: a molecular dynamics study, Biophys. J. 84 (2003) 1507–1517.
[50] M.T. Hyvönen, P.T. Kovanen, Molecular dynamics simulation of sphingomyelin bilayer, J. Phys. Chem. B 107 (2003) 9102–9108.
[51] S.W. Chiu, S. Vasudevan, E. Jakobsson, R.J. Mashl, H.L. Scott, Structure of sphingomyelin bilayers: a simulation study, Biophys. J. 85 (2003) 3624–3635.
[52] T. Róg, M. Pasenkiewicz-Gierula, Cholesterol–sphingomyelin interactions: a molecular dynamics simulation study, Biophys. J. 91 (2006) 3756–3767.
[53] F. Sciortino, P.H. Poole, H.E. Stanley, S. Havlin, Lifetime of the bond network and gel-like anomalies in supercooled water, Phys. Rev. Lett. 64 (1990) 1686–1689.
[54] A.D. Hammerich, V. Buch, An alternative near-neighbor definition of hydrogen bonding in water, J. Chem. Phys. 128 (2008) 111101.
[55] K.S. Bruzik, B. Sobon, G.M. Salamonczyk, Nuclear magnetic resonance study of sphingomyelin bilayers, Biochemistry 29 (1990) 4017–4021.
[56] C.F. Schmidt, Y. Barenholz, T.E. Thompson, A nuclear magnetic resonance study of sphingomyelin in bilayer systems, Biochemistry 16 (1977) 2649–2656.
[57] L.J. Neuringer, B. Sears, F.B. Jungalwala, E.K. Shriver, Difference in orientational order in phospholipid and sphingomyelin bilayers, FEBS Lett. 104 (1979) 173–175.
[58] T. Mehnert, K. Jacob, R. Bittman, K. Beyer, Structure and lipid interaction of *N*-palmitoylsphingomyelin in bilayer membranes as revealed by 2H-NMR spectroscopy, Biophys. J. 90 (2006) 939–946.
[59] D.J. Siminovitch, K.R. Jeffrey, Orientational order in the choline headgroup of sphingomyelin: A ^{14}N-NMR study, Biochim. Biophys. Acta 645 (1981) 270–278.
[60] B. Steinbauer, T. Mehnert, K. Beyer, Hydration and lateral organization in phospholipid bilayers containing sphingomyelin: A ^{2}H-NMR study, Biophys. J. 85 (2003) 1013–1024.
[61] E. Lindahl, O. Edholm, Molecular dynamics simulation of NMR relaxation rates and slow dynamics in lipid bilayers, J. Chem. Phys. 115 (2001) 4938–4950.
[62] R.J. Mashl, H.L. Scott, S. Subramaniam, E. Jakobsson, Molecular simulation of dioleoylphosphatidylcholine lipid bilayers at differing levels of hydration, Biophys. J. 81 (2001) 3005–3015.
[63] P.S. Niemelä, M.T. Hyvönen, I. Vattulainen, Influence of chain length and unsaturation on sphingomyelin bilayers, Biophys. J. 90 (2006) 851–863.
[64] M.O. Jensen, O.G. Mouritsen, Lipids do influence protein function — the hydrophobic matching hypothesis revisited, Biochim. Biophys. Acta 1666 (2004) 205–226.
[65] O.S. Andersen, R.E. Koeppe, Bilayer thickness and membrane protein function: an energetic perspective, Annu. Rev. Biophys. Biomol. Struct. 36 (2007) 107–130.
[66] S. Ollila, M.T. Hyvönen, I. Vattulainen, Polyunsaturation in lipid membranes: dynamic properties and lateral pressure profiles, J. Phys. Chem. B 111 (2007) 3139–3150.
[67] C.F. Schmidt, Y. Barenholz, C. Huang, T.E. Thompson, Monolayer coupling in sphingomyelin bilayer systems, Nature 271 (1978) 775–777.
[68] J.L. Slater, C.H. Huang, Interdigitated bilayer membranes, Prog. Lipid Res. 27 (1988) 325–359.
[69] V. Kiessling, J.M. Crane, L.K. Tamm, Transbilayer effects of raft-like lipid domains in asymmetric planar bilayers measured by single molecule tracking, Biophys. J. 91 (2006) 3313–3326.
[70] C. Wan, V. Kiessling, L.K. Tamm, Coupling of cholesterol-rich lipid phases in asymmetric bilayers, Biochemistry 47 (2008) 2190–2198.
[71] D.W. Allender, M. Schick, Phase separation in bilayer lipid membranes: effects on the inner leaf due to coupling to the outer leaf, Biophys. J. 91 (2006) 2928–2935.
[72] A.J. Wagner, S. Loew, S. May, Influence of monolayer–monolayer coupling on the phase behavior of a fluid lipid bilayer, Biophys. J. 93 (2007) 4268–4277.
[73] I.W. Levin, T.E. Thompson, Y. Barenholz, C. Huang, Two types of hydrocarbon chain interdigitation in sphingomyelin bilayers, Biochemistry 24 (1985) 6282–6286.
[74] C. Huang, J.T. Mason, Structure and properties of mixed-chain phospholipid assemblies, Biochim. Biophys. Acta 864 (1986) 423–470.
[75] P.R. Maulik, D. Atkinson, G.G. Shipley, X-ray scattering of vesicles of *N*-acyl sphingomyelins: determination of bilayer thickness, Biophys. J. 50 (1986) 1071–1077.
[76] S.A. Shkulipa, W.K. den Otter, W.J. Briels, Surface viscosity, diffusion, and intermonolayer friction: simulating sheared amphiphilic bilayers, Biophys. J. 89 (2005) 823–829.
[77] D. Huster, H.A. Scheidt, K. Arnold, A. Herrmann, P. Müller, Desmosterol may replace cholesterol in lipid membranes, Biophys. J. 88 (2005) 1838–1844.
[78] J.A. Urbina, S. Pekerar, H.B. Le, J. Patterson, B. Montez, E. Oldfield, Molecular order and dynamics of phosphatidylcholine bilayer membranes in the prescence of cholesterol, ergosterol and lanosterol: a comparative study using ^{2}H-, ^{13}C- and ^{31}P-NMR spectroscopy, Biochim. Biophys. Acta 1238 (1995) 163–176.
[79] Y.W. Hsueh, M.T. Chen, P.J. Patty, C. Code, J. Cheng, B.J. Frisken, M. Zuckermann, J. Thewalt, Ergosterol in POPC membranes: physical proerties and comparison with structurally similar sterols, Biophys. J. 92 (2007) 1606–1615.
[80] I. Schuler, A. Milon, Y. Nakatani, G. Ourisson, A.M. Albrecht, P. Benveniste, M.A. Hartmann, Differential effects of plant sterols on water permeability and on acyl chain ordering of soybean phosphatidylcholine bilayers, Proc. Natl. Acad. Sci. U. S. A. 88 (1991) 6926–6930.
[81] K.K. Halling, J.P. Slotte, Membrane properties of plant sterols in phospholipid bilayers as determined by differential scanning calorimetry, resonance energy transfer and detergent-induced solubilization, Biochim. Biophys. Acta 1664 (2004) 161–171.
[82] A.M. Smondyrev, M. Berkowitz, Molecular dynamics simulation of the structure of dimyristoylphosphatidylcholine bilayers with cholesterol, ergosterol, and lanosterol, Biophys. J. 80 (2001) 1649–1658.
[83] Z. Cournia, G.M. Ullmann, J.C. Smith, Differential effects of cholesterol, ergosterol and lanosterol on dipalmitoyl phosphatidylcholine membrane: a molecular dynamics simulation study, J. Phys. Chem. B 111 (2007) 1786–1801.
[84] S. Vainio, M. Jansen, M. Koivusalo, T. Róg, M. Karttunen, I. Vattulainen, E. Ikonen, Significance of sterol structural specifity. Desmosterol cannot replace cholesterol in lipid rafts, J. Biol. Chem. 281 (2006) 348–355.
[85] T. Róg, I. Vattulainen, M. Jansen, E. Ikonen, M. Karttunen, Comparison of cholesterol and its direct precursors along the biosynthetic pathway: effects of cholesterol, desmosterol and 7-dehydrocholesterol on saturated and unsaturated lipid bilayers, J. Chem. Phys. (in press).
[86] J. Czub, M. Baginski, Comparative molecular dynamics study of lipid memranes containing cholesterol and ergosterol, Biophys. J. 90 (2006) 2368–2382.
[87] T. Róg, M. Pasenkiewicz-Gierula, I. Vattulainen, M. Karttunen, What happens if cholesterol is made smoother: importance of methyl substituents in cholesterol ring structure on phosphatidylcholine–sterol interaction, Biophys. J. 92 (2007) 3346–3357.
[88] S. Pöyry, T. Róg, M. Karttunen, I. Vattulainen, Significance of cholesterol methyl groups, J. Phys. Chem. B 112 (2008) 2922–2929.
[89] J. Aittoniemi, P.S. Niemelä, M.T. Hyvönen, M. Karttunen, I. Vattulainen, Insight into the putative specific interactions between cholesterol, sphingomyelin and palmitoyl-oleoyl phosphatidylcholine, Biophys. J. 92 (2007) 1125–1137.
[90] Z. Zhang, S.Y. Bhide, M.L. Berkowitz, Molecular dynamics simulations of bilayers containing mixtures of sphingomyelin with cholesterol and phosphatidylcholine with cholesterol, J. Phys. Chem. B 111 (2007) 12888–12897.
[91] G.A. Khelashvili, H.L. Scott, Combined Monte Carlo and molecular dynamics simulation of hydrated 18:0 sphingomyelin–cholesterol lipid bilayers, J. Chem. Phys. 120 (2004) 9841–9847.
[92] S.Y. Bhide, Z. Zhang, M.L. Berkowitz, Molecular dynamics simulations of SOPS and sphingomyelin bilayers containing cholesterol, Biophys. J. 92 (2007) 1284–1295.
[93] P.S. Niemelä, S. Ollila, M.T. Hyvönen, M. Karttunen, I. Vattulainen, Assessing the nature of lipid rafts, PLoS Comput. Biol. 3 (2007) 304–312.
[94] M. Bachar, P. Brunelle, D.P. Tieleman, A. Rauk, Molecular dynamics simulation of a polyunsaturated lipid bilayer susceptible to lipid peroxidation, J. Phys. Chem. B 108 (2004) 7170–7179.
[95] J. Aittoniemi, T. Róg, P. Niemelä, M. Pasenkiewicz-Gierula, M. Karttunen, I. Vattulainen, Tilt: major factor in sterols' ordering capability in membranes, J. Phys. Chem. B 110 (2006) 25562–25564.
[96] S.A. Pandit, S. Vasudevan, S.W. Chiu, R.J. Mashl, E. Jakobsson, H.L. Scott, Sphingomyelin–cholesterol domains in phospholipid membranes: atomistic simulation, Biophys. J. 87 (2004) 1092–1100.
[97] J. Huang, G.W. Feigenson, A microscopic interaction model of maximum solubility of cholesterol in lipid bilayers, Biophys. J. 76 (1999) 2142–2157.
[98] Z. Zhang, L. Lu, M.L. Berkowitz, Energetics of cholesterol transfer between lipid bilayers, J. Phys. Chem. B 112 (2008) 3807–3811.
[99] H.A. Rinia, M.M.E. Snel, J.P.J.M. van der Eerden, B. de Kruijff, Visualizing detergent resistant domains in model membranes with atomic force microscopy, FEBS Lett. 501 (2001) 92–96.
[100] T.J. McIntosh, X-ray diffraction to determine the thickness of raft and nonraft bilayers, Methods Mol. Biol. 398 (2007) 221–230.
[101] A. Filippov, G. Orädd, G. Lindblom, Sphingomyelin structure influences the lateral diffusion and raft formation in lipid bilayers, Biophys. J. 90 (2006) 2086–2092.
[102] N. Kučerka, S. Tristram-Nagle, J.F. Nagle, Structure of fully hydrated fluid phase lipid bilayers with monounsaturated chains, J. Membr. Biol. 208 (2005) 193–202.
[103] M. Patra, E. Salonen, E. Terama, I. Vattulainen, R. Faller, B.W. Lee, J. Holopainen, M. Karttunen, Under the influence of alcohol: The effect of ethanol and methanol on lipid bilayers, Biophys. J. 90 (2006) 1121–1135.
[104] E. Lindahl, O. Edholm, Mesoscopic undulations and thickness fluctuations in lipid bilayers from molecular dynamics simulations, Biophys. J. 79 (2000) 426–433.
[105] E. Evans, W. Rawicz, Entropy driven tension and bending elasticity in condensed-fluid membranes, Phys. Rev. Lett. 64 (1990) 2094–2097.
[106] W. Rawicz, K.C. Olbrich, T. McIntosh, D. Needham, E. Evans, Effect of chain length and unsaturation on elasticity of lipid bilayers, Biophys. J. 79 (2000) 328–339.
[107] D. Needham, T.J. McIntosh, E. Evans, Thermomechanical and transition properties of dimyristoylphosphatidylcholine/cholesterol bilayers, Biochemistry 27 (1988) 4668–4673.
[108] D. Needham, R.S. Nunn, Elastic deformation and failure of lipid bilayer membranes containing cholesterol, Biophys. J. 58 (1990) 997–1009.
[109] T. Murtola, T. Róg, E. Falck, M. Karttunen, I. Vattulainen, Transient ordered domains in single-component phospholipid bilayers, Phys. Rev. Lett. 97 (2006) 238102.
[110] R.S. Cantor, The influence of membrane lateral pressures on simple geometric models of protein conformational equilibria, Chem. Phys. Lipids 101 (1999) 45–56.
[111] J. Gullingsrud, K. Schulten, Lipid bilayer pressure profiles and mechanosensitive channel gating, Biophys. J. 86 (2004) 3496–3509.
[112] R.S. Cantor, The lateral pressure profile in membranes: a physical mechanism of general anesthesia, Biochemistry 36 (1997) 2339–2344.
[113] R.G. Eckenhoff, Promiscuous ligands and attractive cavities. How do the inhaled anesthetics work? Mol. Interv. 1 (2001) 258–268.
[114] E. Lindahl, O. Edholm, Spatial and energetic–entropic decomposition of surface tension in lipid bilayers from molecular dynamics simulations, J. Chem. Phys. 113 (2000) 3882–3893.
[115] M. Patra, Lateral pressure profiles in cholesterol–DPPC bilayers, Eur. Biophys. J. 35 (2005) 79–88.
[116] J. Sonne, F.Y. Hansen, G.H. Peters, Methodological problems in pressure profile calculations for lipid bilayers, J. Chem. Phys. 122 (2005) 124903.

[117] S. Ollila, Lateral pressure profile calculations of lipid membranes from atomic scale molecular dynamics simulations, Master's thesis, Helsinki Univ. Tech. (2006).
[118] S. Sukharev, S.R. Durell, H.R. Guy, Structural models of the MscL gating mechanism, Biophys. J. 81 (2001) 917–936.
[119] S.I. Sukharev, W.J. Sigurdson, C. Kung, F. Sachs, Energetic and spatial parameters for gating of the bacterial large conductance mechanosensitive channel, MscL, J. Gen. Physiol. 113 (1999) 525–540.
[120] J.R. Lewis, D.S. Cafiso, Correlation of the free energy of a channel-forming voltage-gated peptide and the spontaneous curvature of bilayer lipids, Biochemistry 38 (1999) 5932–5938.
[121] D. Allende, S.A. Simon, T.J. McIntosh, Melittin-induced bilayer leakage depends on lipid material properties: evidence for toroidal pores, Biophys. J. 88 (2005) 1828–1837.
[122] S. Safran, Statistical Thermodynamics of Surfaces, Interfaces and Membranes, Addison-Wesley, New York, 1994.
[123] T. Murtola, E. Falck, M. Patra, M. Karttunen, I. Vattulainen, Coarse-grained model for phospholipid/cholesterol bilayer, J. Chem. Phys. 121 (2004) 9156–9165.
[124] T. Murtola, E. Falck, M. Karttunen, I. Vattulainen, Coarse-grained model for phospholipid/cholesterol bilayer employing inverse Monte Carlo with thermodynamic constraints, J. Chem. Phys. 126 (2007) 075101.
[125] G.A. Khelashvili, S.A. Pandit, H.L. Scott, Self-consistent mean field model based on molecular dynamics: application to lipid–cholesterol bilayers, J. Chem. Phys. 123 (2005) 34910.
[126] S.A. Pandit, S.W. Chiu, E. Jakobsson, A. Grama, H.L. Scott, Cholesterol surrogates: a comparison of cholesterol and 16:0 ceramide in POPC bilayers, Biophys. J. 92 (2007) 920–927.
[127] S.J. Marrink, A.H. de Vries, A.E. Mark, Coarse grained model for semiquantitative lipid simulations, J. Phys. Chem. B 108 (2004) 750–760.
[128] S.J. Marrink, A.H. de Vries, T.A. Harroun, J. Katsaras, S.R. Wassall, Cholesterol shows preference for the interior of polyunsaturated lipid membranes, J. Am. Chem. Soc. 130 (2007) 10–11.
[129] R. Faller, S.J. Marrink, Simulation of domain formation in DLPC–DSPC bilayers, Langmuir 20 (2004) 7686–7693.
[130] S.J. Marrink, J. Risselada, A.E. Mark, Simulation of gel phase formation and melting in lipid bilayers using a coarse grained model, Chem. Phys. Lipids 135 (2005) 223–244.
[131] S. Baoukina, L. Monticelli, S.J. Marrink, D.P. Tieleman, Pressure-area isotherm of a lipid monolayer from molecular dynamics simulations, Langmuir 23 (2007) 12617–12623.
[132] A.A. Gurtovenko, I. Vattulainen, Lipid transmembrane asymmetry and intrinsic membrane potential: two sides of the same coin, J. Am. Chem. Soc. 129 (2007) 5358.
[133] T. Róg, I. Vattulainen, M. Karttunen, Modelling glycolipids: take one, Cell. Mol. Biol. Lett. 10 (2005) 625–630.
[134] T. Róg, I. Vattulainen, A. Bunker, M. Karttunen, Glycolipid membranes through atomistic simulations: effect of glucose and galactose head groups on lipid bilayer properties, J. Phys. Chem. B 111 (2007) 10146–10154.